Geochemistry, Geophysics, Geosystems®

RESEARCH ARTICLE
10.1029/2022GC010766

Key Points:

- We explore the behavior of dual-clumped and fluid-inclusion isotope paleothermometers during thermal alteration
- Different conditions during diagenesis may result in discrepant paleotemperature estimates, which may be used to identify altered records
- Hand-drilling belemnites produces sufficient heat to reset paleotemperatures, but the heat during analysis of fluid inclusions does not

Supporting Information:

Supporting Information may be found in the online version of this article.

Correspondence to:

P. Staudigel,
staudigel@em.uni-frankfurt.de

Citation:

Staudigel, P., Davies, A. J., Bernecker, M., Tagliavento, M., van der Lubbe, H. J. L., Nooitgedacht, C., et al. (2023). Fingerprinting kinetic isotope effects and diagenetic exchange reactions using fluid inclusion and dual-clumped isotope analysis. *Geochemistry, Geophysics, Geosystems*, *24*, e2022GC010766. https://doi.org/10.1029/2022GC010766

Received 4 NOV 2022
Accepted 20 JAN 2023
Corrected 12 APR 2023

This article was corrected on 12 APR 2023. See the end of the full text for details.

Author Contributions:

Conceptualization: J. Fiebig
Data curation: A. J. Davies, M. Bernecker, J. Fiebig
Funding acquisition: J. Fiebig
Investigation: A. J. Davies, H. J. L. van der Lubbe, C. Nooitgedacht, N. Looser, S. M. Bernasconi, H. Vonhof, J. Fiebig

Fingerprinting Kinetic Isotope Effects and Diagenetic Exchange Reactions Using Fluid Inclusion and Dual-Clumped Isotope Analysis

P. Staudigel[1], A. J. Davies[1], M. Bernecker[1], M. Tagliavento[1], H. J. L. van der Lubbe[2], C. Nooitgedacht[2], N. Looser[3], S. M. Bernasconi[3], H. Vonhof[4], and J. Fiebig[1]

[1]Institute of Geosciences, Goethe University Frankfurt, Frankfurt am Main, Germany, [2]Department of Earth Sciences, Vrije Universiteit Amsterdam, Amsterdam, The Netherlands, [3]Geological Institute, ETH-Zurich, Zurich, Switzerland, [4]Max Planck-Institut für Chemie, Mainz, Germany

Abstract Geochemical analyses of carbonate minerals yield multiple parameters which can be used to estimate the temperature and water composition at which they formed. Analysis of fluid trapped in minerals is a potentially powerful tool to reconstruct paleotemperatures as well as diagenetic and hydrothermal processes, as these could represent the parent fluid. Internal fluids play important roles during the alteration of carbonate fossils, lowering energetic barriers associated with resetting of clumped isotopes, as well as mediating the transport of elements during diagenesis. Here, we explore the behavior of the Δ_{47}–Δ_{48} "dual-clumped" isotope thermometer during fluid-carbonate interaction and demonstrate that it is highly sensitive to the water/carbonate ratio, behaving as a linear system in "rock buffered" alteration, and as a decoupled system in water-dominated systems due to non-linear mixing effects in Δ_{48}. Dry heating experiments show that the extrapolated "heated" end-member is indistinguishable from the predicted Δ_{47} and Δ_{48} value expected for the experimental temperature. Furthermore, we evaluate two common laboratory sampling methods for their ability to thermally alter samples. We find that the temperature of the commonly used crushing cells used to vapourize water for fluid inclusion $\delta^{18}O$ analyses is insufficient to cause fluid-carbonate oxygen isotope exchange, demonstrating its suitability for analyses of fluid inclusions in carbonates. We also find that belemnites sampled with a hand-drill yield significantly warmer paleotemperatures than those sampled with mortar and pestle. We conclude that thermally-driven internal fluid-carbonate exchange occurs indistinguishably from isotopic equilibrium, limited by the extent to which internal water and carbonate can react.

Plain Language Summary Carbonate minerals contain multiple, independent, chemical and isotopic parameters which can be used to calculate the temperature at which the mineral formed. If these proxies agree with one another, it has been confidently assumed that the temperature is indeed genuine. Here, we investigate three such parameters and show how they record kinetic processes during mineral formation, as well as thermally-driven processes which may alter a climate record. We find that this method could potentially be used to study the kinetic factors at play during biomineralization, even if the "true" temperature is unknown. We also find that some thermal processes result in all three parameters agreeing with one another. Because thermal alteration poses a potential dilemma for climate researchers, we investigate two common laboratory preparation techniques that involve heating a sample before analysis: drilling and heating sample for fluid inclusion analysis. We find that the heat of a drill is sufficient to facilitate these reactions, and potentially imparts a warm bias onto paleotemperatures, however the apparatus used for analyzing fluid inclusions does not appear to significantly alter the material. We conclude our approach using fluid inclusion analysis and dual-clumped isotopes has the potential to resolve many ambiguities in interpreting climate records.

1. Introduction

Carbonate clumped isotope analysis measures the distribution of multiply-substituted isotopologues of CO_2 (e.g., $^{13}C^{18}O^{16}O$ or $^{12}C^{18}O^{18}O$) liberated from carbonate minerals when acidified (Ghosh et al., 2006). The abundance of the rarer multiply-substituted isotopologues is higher than that expected in a stochastic distribution of isotopes, an effect which diminishes at higher temperatures, making it a useful paleothermometer, typically expressed in "delta notation" as follows.

$$\Delta_x = \left[\frac{{}^{x}R_{\text{measured}}}{{}^{x}R_{\text{stochastic}}} - 1\right] \times 1000‰ \quad (1)$$

Methodology: A. J. Davies, M. Bernecker, H. J. L. van der Lubbe, C. Nooitgedacht, N. Looser, S. M. Bernasconi, H. Vonhof, J. Fiebig
Project Administration: J. Fiebig
Resources: A. J. Davies, M. Bernecker
Software: M. Bernecker
Supervision: J. Fiebig
Visualization: J. Fiebig
Writing – original draft: A. J. Davies, M. Bernecker, H. J. L. van der Lubbe, C. Nooitgedacht, N. Looser, S. M. Bernasconi, H. Vonhof, J. Fiebig
Writing – review & editing: A. J. Davies

The enrichment of clumped isotope bonds does not behave in a conservative manner (i.e., it cannot saturate a fluid and become "rock buffered" with respect to Δ_{47}) and clumped isotope bonds can be reset via internal exchange processes without requiring exchange with external media (Hemingway & Henkes, 2021; Passey & Henkes, 2012; Stolper & Eiler, 2015). As a result of this non-conservative behavior, clumped isotopes are suitable for studying isotopic exchange reactions between carbonate and water even in systems with low water/carbonate ratios where bulk isotope partitioning tends to become rock-buffered (Nooitgedacht, van der, Lubbe, de, et al., 2021; Ryb & Eiler, 2018; Staudigel & Swart, 2019; Veillard et al., 2019).

Recent advances in mass spectrometry have enabled accurate measurement of the Δ_{48} value (Fiebig et al., 2019; Swart et al., 2021), which—in combination with Δ_{47}—provides independent constraints of kinetic effects (Bajnai et al., 2020). This is possible because the ^{18}O-^{18}O (the main contributor to Δ_{48}) and ^{13}C-^{18}O (the main contributor to Δ_{47}) substituted isotopologues are affected by different kinetic limitations, and thus in systems with disequilibrium carbonate pools, the combined measurement of both isotopologues can be used to constrain the factors affecting disequilibrium (Guo, 2020; Watkins & Devriendt, 2022).

Hydrothermal alteration of carbonate fossils alters skeletal chemistry via exchange reactions between fluids and the solid phase, where the relative contributions of internal and external fluid can vary (Banner & Hanson, 1990; Pederson et al., 2020; Wardlaw et al., 1978). Internal fluids play an important role lowering the energetic barriers of clumped isotope resetting (Brenner et al., 2018; Nooitgedach, van der Lubbe, Ziegler, & Staudigel, 2021), if these internal fluids form an inter-connected network, they can mediate the transport of ions into and out of a fossil (Staudigel et al., 2022; Wardlaw et al., 1978). Internal water may be comprised of several different reservoirs, such as "true" fluid inclusions (Figures 1a and 1b), or organic-derived water which can be released during heating (Figures 1c and 1d) (Gaffey et al., 1991). Water liberated from structural organic components can have many sources and form at different temperatures (Figure 1c). Hydrated proteins will denature and expel water at temperatures under 100°C (Wortmann et al., 2012). At temperatures exceeding 100°C, free amino acids can spontaneously polymerize, yielding additional water (Pedreira-Segade et al., 2019). The decomposition of organic compounds can provide an additional source of internal organic-bound water. If no external fluid exists, or some limitation is placed on exchange between internal and external water reservoirs, then the interaction between internal water and carbonate represents the lowest possible water/carbonate ratios for any natural exchange process, typically with only a few wt% of internal water available for exchange (Gaffey, 1988). The observation that, even in this extremely rock-dominated system, clumped isotopes can be significantly overprinted, as demonstrated by Nooitgedacht, van der, Lubbe, de, et al. (2021) and Looser et al. (2023), is therefore one of great importance.

To quantitatively describe diagenetic exchange reactions, it is critical to understand the dynamics of internal fluid-carbonate exchange. Dry-heating experiments with sclerosponge *Ceratoporella nicholsonii* have demonstrated that aragonitic $\delta^{18}O$ and Δ_{47} will change with moderate heating, even if this occurs in a vacuum and before conversion to calcite (Staudigel & Swart, 2016). Aragonite converted to calcite by heating under normal atmospheric conditions, or in isotopically labeled CO_2 atmosphere, can exchange C and O isotopes between gaseous CO_2 and the CO_3^{2-} of the mineral during the aragonite-calcite transition (Staudigel & Swart, 2016). Looser et al. (2023), have observed thermal resetting of belemnite Δ_{47} proceeds at higher rates and at temperatures lower than those required for optical calcite, which is accompanied with a change in belemnite $\delta^{18}O$, suggesting that this is due to exchange between carbonate and internal water. These experiments demonstrate that the original paleotemperature recorded in carbonate minerals could be more rapidly reset than would be expected from purely solid-state reordering during heating/burial even if water/carbonate ratio is extremely low, and at temperatures lower than those considered necessary to facilitate solid-state bond reordering within the carbonate mineral (Henkes et al., 2014; Passey & Henkes, 2012). At lower temperatures (<375°C for aragonite, <420°C for belemnite), these experiments rarely fully reset the carbonate mineral's Δ_{47} value over the experimental duration to predicted thermodynamic equilibrium, with Δ_{47} values instead being more positive than the predicted equilibrium value (Staudigel & Swart, 2016).

Heating from laboratory handling (e.g., drilling) has been demonstrated to produce sufficient temperature to convert aragonite to calcite and initiate related clumped isotope resetting (Staudigel & Swart, 2016). Considering heating-induced fluid-carbonate exchange has been observed in experiments at 125°C over days (Staudigel & Swart, 2016) and over months at 100°C (Ritter et al., 2017), it is important to critically evaluate the heating used during fluid inclusion analysis (up to 150°C; Dennis et al., 2001). If oxygen exchange occurs during analysis, then it would effectively reset the fluid $\delta^{18}O$ values thus invalidating it as a viable analytical method.

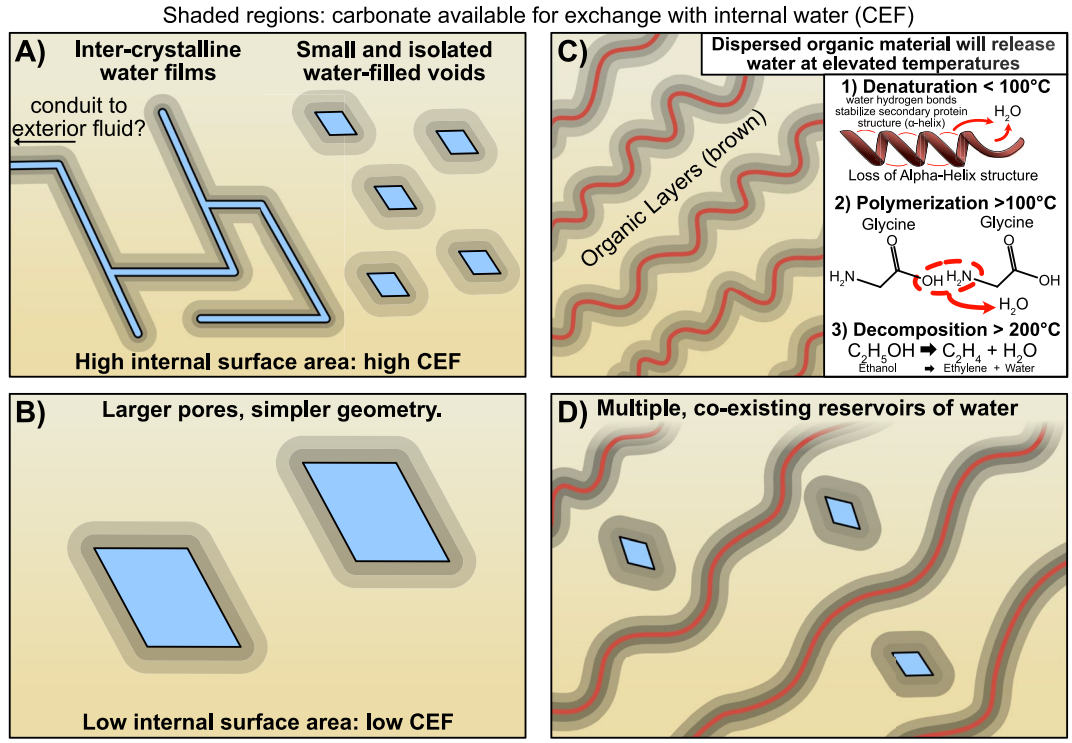

Figure 1. Diagram showing different possible structures and sources for internal water in carbonates. (a) Dispersed internal fluids with a high internal surface area. (b) Larger fluid inclusions with lower internal surface area. (c) Organic-associated water (d) mixture of organic-associated and "classic" fluid inclusions.

Experimentally observed partial resetting of clumped isotopes implies a limitation for the extent of secondary equilibration. Models for physical limitation of isotopic resetting assume that full equilibrium with the fluid is attained, but that only a fraction of carbonate (the Carbonate Exchange Fraction: CEF) is available for exchange, while the remaining carbonate retains its original composition (Nooitgedacht, van der, Lubbe, de, et al., 2021). Variation in CEF can account for different relationships between $\delta^{18}O$ and Δ_{47} (Figure 2a). CEF variation could potentially reflect different structures of pores, possibly with variable surface area (Figures 1a and 1b) or sources of internal water (Figures 1c and 1d). Analysis of fluid inclusion $\delta^{18}O$ and the corresponding carbonate Δ_{47} values for dry-heating experiments were able to establish a relationship between fluid-carbonate exchange and Δ_{47} resetting (Nooitgedacht, van der, Lubbe, de, et al., 2021), but apparently this system cannot be fully described by the CEF model, as $T\alpha_{c\text{-}w}$ and $T\Delta_{47}$ values of heated biogenic carbonates plot in a mathematically implausible region if all fluids are available for exchange (Figure 2a). Because of this, additional constraint is required to describe this system. In this study, we expand upon the CEF model developed by Nooitgedacht, van der, Lubbe, de, et al. (2021); modifying it such that it allows for Water Exchange Fractions (WEF) and expanding the output to include Δ_{48} values. We supplement the Nooitgedach, van der Lubbe, Ziegler, and Staudigel (2021) fluid inclusion values with analyses of heated and unheated belemnites. These data will be used to study the kinetic effects present during mineral formation and during thermal alteration and will be used to explore methods for fingerprinting these effects in "unknown" samples.

2. Materials and Methods

2.1. Experimental Materials

Four sample types are discussed in this study, a modern coral (*Montastrea annularis*; VUA collection), a modern giant clam (*Hippopus porceleanus*; antique trade), an abiogenic single-crystal "Moroccan Aragonite" (Tazouta, Morocco), and belemnites taken from Latest Cretaceous in Norfolk and Middle Jurassic in Wiltshire (Looser et al., 2023; Vickers et al., 2021). The first three samples are the same sample materials as those analyzed for fluid inclusions and conventional clumped isotopes by Nooitgedach, van der Lubbe, Ziegler and Staudigel (2021).

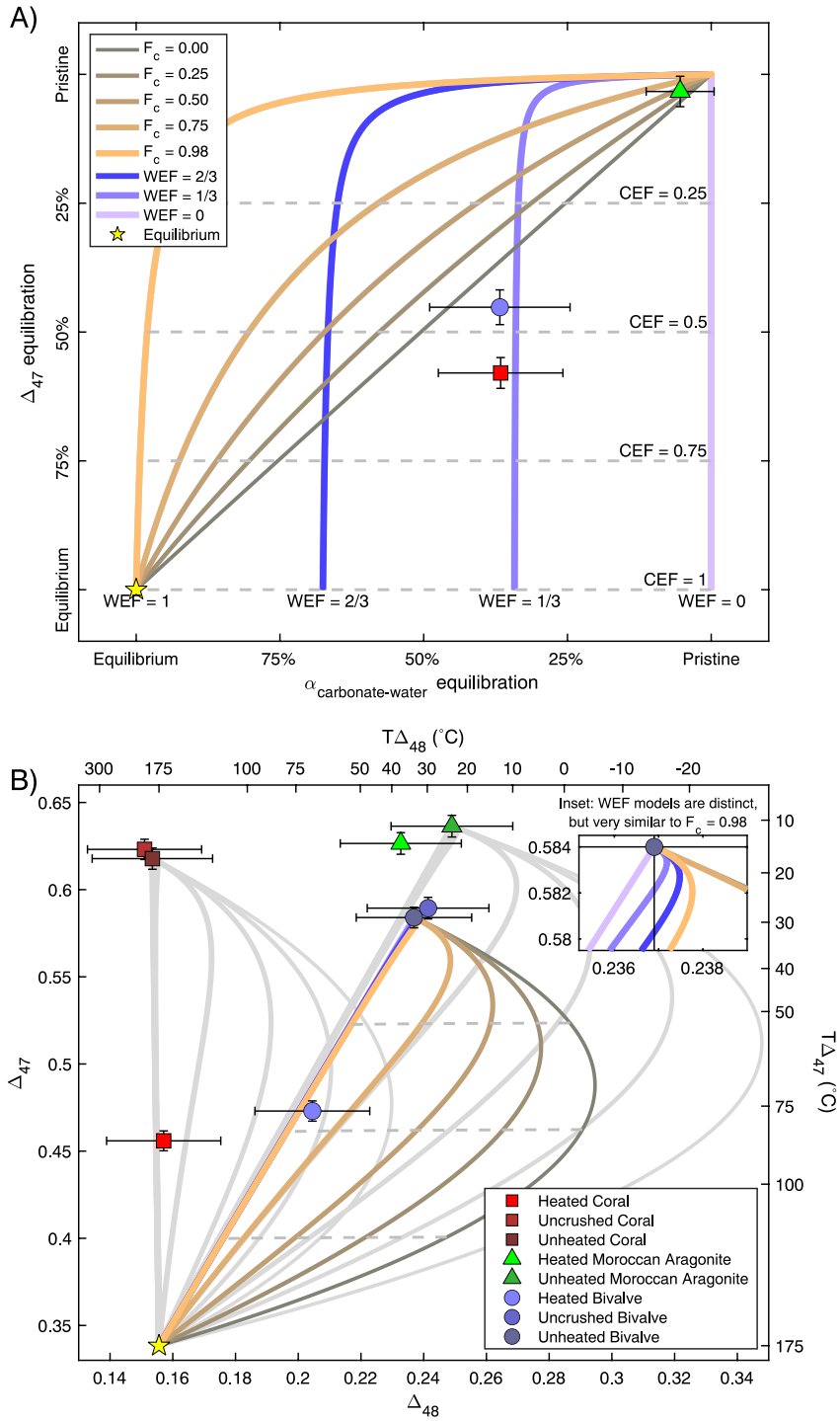

Figure 2. Mass-balance model results for closed-system carbonate-fluid exchange (Carbonate Exchange Fraction [CEF] Model) with variable fractions of water available for exchange (WEF, blue lines). (a) comparison of the degree of equilibration of $\alpha_{c\text{-}w}$ and Δ_{47} in different models. Measured data for heated samples are shown as symbols, data are rescaled such that all unheated points are in the upper right corner (labeled "pristine") and the bottom left corner constitutes equilibrium at 175°C. Note that the original CEF model (Nooitgedach, van der Lubbe, Ziegler, & Staudigel, 2021) cannot explain some data (bivalve and coral) with any water/rock ratio necessitating the additional WEF term (see Section 4.4).

Error bars are adjusted such that they represent the root of sum squares of the two measured values ($\sigma_{sum} = \sqrt{\sigma_a^2 + \sigma_b^2}$). (b) measured Δ_{47} and Δ_{48} values for all samples, with CEF/WEF models shown for each starting composition (Unheated). Inset shows difference between WEF variable models, focused on the unheated bivalve value. All panels of this Figure use the same color code and symbols as shown in the legends.

Novel fluid inclusion analyses are presented for heated and unheated Cretaceous belemnite rostra. Dual-clumped isotope measurements are presented for a series of heating experiments conducted by Looser et al. (2023) using Jurassic belemnites. Additionally, four Cretaceous belemnites have been analyzed using different sampling methods.

2.2. Experimental Treatments

The aragonitic samples (all samples excluding belemnites) were treated one of three ways: termed "heated" (175°C for 90 min, then analyzed for fluid inclusions at 110°C), "unheated" (analyzed for fluid inclusions at 110°C), and "uncrushed" (simply powdered in mortar and pestle then analyzed for clumped isotopes). Note that we are using the terminology used by Nooitgedach, van der Lubbe, Ziegler, and Staudigel (2021), however both the "heated" and "unheated" samples were, in fact heated to 110°C, whereas the "uncrushed" samples were never heated to such a degree. The purpose of the "uncrushed" treatment is to determine the suitability of the commonly used crushing cells, (hereafter referred to as a "crusher apparatus") for fluid inclusion water stable isotope analysis of biogenic carbonates. The belemnite samples were heated at various temperatures for variable duration shown in Table 1.

In a separate experiment, 500 mg pieces of Maastrichtian belemnites from Norfolk (BNLM-2 and BNLM-11) were heated to 360°C for 2 hr, these pieces and unheated equivalents were then analyzed for fluid inclusions' $\delta^{18}O$ values. Both unheated and heated belemnite fragments were analyzed for their dual clumped isotope compositions (Δ_{47} and Δ_{48}).

An additional experiment was conducted to evaluate the effects of drill-induced heating. Four specimens of Cretaceous belemnites were selected and sampled using both a mortar and pestle and hand-drill. Roughly >100 mg of powder was produced with each method, which was subsequently analyzed for Δ_{47} and Δ_{48}.

2.3. Clumped Isotope Analyses

Clumped isotope analyses were conducted at Goethe University Frankfurt, using the instrumental setup and data evaluation procedure presented by Fiebig et al. (2019, 2021). Data evaluation was modified after Davies et al. (2022). Briefly, all raw δ^{45}–δ^{49} and Δ_{47}–Δ_{48} values were corrected for the negative pressure baseline effect using intensities read in by the half mass cup 47.5 multiplied by iteratively determined, session and mass specific scaling factors, such that residual slopes of equilibrated gas standards in δ^i-Δ_i-space (i = 47, 48, 49) are indistinguishable from zero (Fiebig et al., 2021). Background corrected raw data was then converted to the CDES 90 using D47crunch (Daëron, 2021) applying assigned Δ_{47} and Δ_{48} values of 0.9196 and 0.345‰, respectively, for CO_2 equilibrated at 25°C, and values of 0.0266 and 0 ‰ for CO_2 equilibrated at 1,000°C. The data were collected in three analytical sessions (September–December 2021, January–April 2022 July–October 2022). Since all of the replicates of a given sample were measured in the same session, data was processed using the "Individual session" option of D47crunch. Final Δ_{47} (CDES 90) and Δ_{48} (CDES 90) data is reported in Table 1, along with 2 SE uncertainties, based on full error propagation considering standardization errors (Daëron, 2021). Recently, Δ_{47} data has also been reported on the I-CDES scale (Bernasconi et al., 2021), the I-CDES Δ_{47} data are reported in Table 1. However, note that the I-CDES is not available for Δ_{48} yet, and that our Δ_{47}-CDES 90 values are not identical to Δ_{47}-I-CDES values (Davies et al., 2022; Fiebig et al., 2021). We, therefore, consistently refer our Δ_{47} (CDES 90) and Δ_{48} (CDES 90) values to the polynomial best fits presented by Fiebig et al. (2021), who rescaled the equilibrium calcite polynomials of Hill et al. (2014) to fit experimental CDES 90 data.

$$\Delta_{47}\,(\text{CDES 90}) = 1.038 * \left(-5.897 * \frac{1}{T} - 3.521 * \frac{10^3}{T^2} + 2.391 * \frac{10^7}{T^3} - 3.541 * \frac{10^9}{T^4}\right) + 0.1856 \quad (2)$$

$$\Delta_{48}\,(\text{CDES 90}) = 1.028 * \left(+6.002 * \frac{1}{T} - 1.299 * \frac{10^4}{T^2} + 8.996 * \frac{10^6}{T^3} - 7.423 * \frac{10^8}{T^4}\right) + 0.1245 \quad (3)$$

Most samples are analyzed with 8–9 replicates, however some of the samples for the Jurassic heated belemnite only yielded sufficient material for 3 replicate analyses.

Geochemistry, Geophysics, Geosystems

10.1029/2022GC010766

Table 1
Results of Isotopic Analyses

Sample name	N_{clump}	$\delta^{13}C$ (‰ VPDB)	$\delta^{18}O_{carb}$ (‰VPDB)[a]	Δ_{47} (‰ CDES-90)	Δ_{47} (‰ I-CDES)	±2se	$T\Delta_{47}$ (°C)[b]	Δ_{48} (‰ CDES-90)	±2se	$T\Delta_{48}$ (°C)[b]	N_{fluid}	$\delta^{2}H_{water}$ (‰V-SMOW)	±2se	$\delta^{18}O_{water}$ (‰V-SMOW)	±2se	$\alpha_{c\text{-}w}$	±2se	$T\alpha_{c\text{-}w}$ (°C)[c]
Coral—Porites, VU collection																		
Uncrushed	9	−1.98	−4.52	0.623	0.638	0.006	15.6	0.157	0.019	170.8								
Unheated	8	−1.82	−4.53	0.617	0.632	0.006	17.4	0.159	0.020	162.4	4	34.1	4.1	0.8	1.4	1.0254	0.0014	44.7
175°C–2 hr	9	−1.91	−4.96	0.455	0.465	0.006	85.9	0.163	0.019	149.6	4	−13.4	4.7	6.7	1.3	1.0190	0.0013	84.9
Bivalve—Hippopus Porceleanus, mineral trade																		
Uncrushed	8	2.91	−1.36	0.589	0.603	0.007	27.2	0.247	0.020	25.3								
Unheated	9	2.45	−1.62	0.584	0.598	0.006	29.2	0.243	0.020	28.9	4	−38.5	7.3	1.7	2.3	1.0275	0.0024	33.8
175°C–2 hr	9	2.21	−1.93	0.473	0.483	0.006	76.7	0.210	0.019	61.2	4	47.3	4.2	8.5	0.7	1.0203	0.0007	76.1
Abiotic Aragonite—Tazauto Morocco																		
Unheated	8	8.34	−7.74	0.636	0.652	0.007	11.2	0.254	0.020	20.0	4	−54.8	2.5	−8.8	0.6	1.0320	0.0006	12.2
175°C–2 hr	8	8.36	−7.79	0.626	0.641	0.007	14.4	0.237	0.020	33.3	4	−54	9.6	−7.6	1.3	1.0307	0.0014	18.1
Cretaceous Belemnites—Norfolk, UK																		
Unheated	8	1.8	0.56	0.610	0.625	0.007	20.0	0.259	0.022	16.1	4	−44.1	10.2	0.8	3.1	1.0307	0.0032	14.7
360°C–2 hr	8	1.83	0.44	0.369	0.368	0.007	145.5	0.164	0.021	146.8	3	−17.7	26.9	26.6	2.9	1.0046	0.0029	213.8
Jurrasic Belemnites—Wiltshire, UK																		
Unheated	9	2.28	−0.37	0.608	0.620	0.006	20.6	0.243	0.019	28.4								
300°C–2 hr	3	2.04	−0.85	0.541	0.552	0.010	45.3	0.242	0.032	29.5								
300°C–96 hr	4	2.27	−0.99	0.468	0.475	0.008	79.2	0.187	0.028	94.2								
360°C–2 hr	8	2.67	−0.86	0.491	0.500	0.006	67.3	0.229	0.020	40.7								
360°C–2 min	3	2.02	−0.63	0.594	0.606	0.010	25.4	0.266	0.032	11.9								
360°C–96 hr	8	2.52	−0.80	0.370	0.375	0.006	144.7	0.162	0.020	151.7								
420°C–2 hr	7	2.45	−0.87	0.353	0.358	0.007	159.7	0.175	0.021	118.3								
420°C–2 min	6	2.47	−0.85	0.527	0.537	0.007	51.4	0.234	0.023	36.2								
420°C–96 hr	7	2.18	−0.98	0.268	0.270	0.007	285.1	0.155	0.021	177.0								
480°C–2 hr	7	2.57	−1.03	0.265	0.266	0.007	292.7	0.144	0.021	238.2								
480°C–2 min	11	2.18	−0.82	0.451	0.458	0.005	88.1	0.211	0.017	60.4								
480°C–96 hr	10	2.38	−1.00	0.227	0.228	0.006	422.9	0.131	0.018	400.0								
Assorted Belemnites sampled with Drill or Mortar + Pestle																		
LIV3 Drilled	7	0.67	0.53	0.593	0.605	0.007	25.8	0.245	0.021	26.9								
LIV3 M + P	10	0.44	0.70	0.600	0.611	0.006	23.5	0.246	0.018	25.9								
MK4 Drilled	7	1.58	0.95	0.575	0.587	0.007	32.3	0.245	0.021	26.8								
MK4 M + P	10	1.42	1.06	0.606	0.618	0.006	21.4	0.255	0.018	19.1								
SK1 Drilled	8	1.06	0.78	0.580	0.591	0.006	30.6	0.259	0.020	16.3								
SK1 M + P	9	0.84	0.89	0.609	0.622	0.006	20.1	0.262	0.019	14.2								

Table 1
Continued

Sample name	N_{clump}	$\delta^{13}C$ (‰ VPDB)	$\delta^{18}O_{carb}$ (‰ VPDB)[a]	Δ_{47} (‰ CDES-90)	Δ_{47} (‰ I-CDES)	±2se	$T\Delta_{47}$ (°C)[b]	Δ_{48} (‰ CDES-90)	±2se	$T\Delta_{48}$ (°C)[b]	N_{fluid}	$\delta^{2}H_{water}$ (‰ V-SMOW)	±2se	$\delta^{18}O_{water}$ (‰ V-SMOW)	±2se	$\alpha_{c\text{-}w}$	±2se	$T\alpha_{c\text{-}w}$ (°C)[c]
SK7 D	9	0.38	0.57	0.579	0.591	0.006	30.8	0.257	0.019	17.8								
SK7 M + P	8	0.37	0.74	0.602	0.615	0.006	22.8	0.269	0.020	9.6								

[a]Carbonate values are corrected for acid digestion following the acid fractionation factors of Kim et al. (2007). [b]Clumped isotope paleotemperatures determined using the polynomial presented by Fiebig et al. (2021). [c]$T\alpha_{c\text{-}w}$ values are calculated for aragonite following Kim et al. (2007) and for calcite following Kim and O'Neil (1997).

2.4. Fluid Inclusion Analysis

Fluid inclusion $\delta^{18}O$ values for the aragonite specimens are taken from Nooitgedach, van der Lubbe, Ziegler, and Staudigel (2021), which were analyzed at the Earth Science Stable Isotope Laboratory of Vrije Universiteit Amsterdam (VU), the Netherlands, following methodology of Vonhof et al. (2006) with modifications outlined by Nooitgedacht, van der, Lubbe, de, et al. (2021) and Nooitgedach, van der Lubbe, Ziegler, and Staudigel (2021). One set of heated and unheated Cretaceous belemnites were analyzed at VU, and one set from the same formation was analyzed at the Max Planck Institute in Mainz, Germany (de Graaf et al., 2020). Both labs' methodology involves heating sample to 110°C for 1–2 hr, before crushing with a manually-actuated crusher apparatus, releasing water into a carrier gas, which is then analyzed for $\delta^{2}H$ and $\delta^{18}O$. Water isotope standards are injected into a port of the crusher apparatus, and are afterward treated identically to water released from a crushed sample. Due to belemnite samples being unexpectedly dry, only half the number of replicate analyses were possible in each session, and thus the results from BNLM-2 and BNLM-11 are treated as a single sample in subsequent statistics, with carbonate values for BNLM-2 being presented in Table 1, both carbonate isotope results are available in Supporting Information S1. We support this choice by emphasizing the indistinguishable $\delta^{13}C$, $\delta^{18}O$ Δ_{47}, and Δ_{48} values for both specimens. In samples where $\delta^{18}O$ values are available for both the carbonate and internal fluids, the equilibrium fractionation of oxygen isotopes between these two phases is defined in Equation 4.

$$\alpha_{c-w} = \frac{{}^{18}R_{\text{carbonate}}}{{}^{18}R_{\text{water}}} = \frac{\left(\delta^{18}O_{\text{carbonate}} + 1,000\right)}{\left(\delta^{18}O_{\text{water}} + 1,000\right)} \tag{4}$$

The uncertainty for fluid inclusion isotopes is calculated based on replicate analyses of sub-samples taken from similar specimens (usually same, except in case of belemnites BNLM-2 and BNLM-11, which are treated as one sample). Crystallization temperatures ($T\alpha_{c\text{-}w}$) are estimated using the measured $\delta^{18}O$ values of fluid and carbonate to calculate $\alpha_{c\text{-}w}$ and subsequently inverting published temperature-$\alpha_{c\text{-}w}$ relationships for aragonite (Kim et al., 2007) and calcite (Kim & O'Neil, 1997).

2.5. A Mass-Balance Model for Internal Fluid-Carbonate Exchange

Analyses of carbonates and fluids that have undergone exchange at variable temperatures have revealed that internal fluids often can only exchange with some fraction of carbonate after it is formed (CEF), and thus bulk analyses of carbonates often yield disequilibrium $\delta^{18}O$ and Δ_{47} values (Nooitgedacht, van der, Lubbe, de, et al., 2021; Uemura et al., 2019). The CEF isotope-balance model used to describe results was defined following Nooitgedacht, van der, Lubbe, de, et al. (2021), where the $^{18}O/^{16}O$ ratio of fluid inclusions after heating was defined as follows.

$${}^{18}R^{\text{heated}}_{\text{fluid}} = \frac{{}^{18}R^{\text{initial}}_{\text{carbonate}} * F_c * \text{CEF} + {}^{18}R^{\text{initial}}_{\text{fluid}} * (1 - F_c)}{F_c * \text{CEF} + (1 - F_c) * \alpha_{c-w}(T)} \tag{5}$$

This model assumes that isotopic exchange between carbonate and water occurs at equilibrium, governed by a temperature-specific fractionation factor (Equation 4). F_c is the molar fraction of oxygen in carbonate (with respect to the carbonate-fluid system) and CEF represents the fraction of carbonate available for exchange with the internal fluid. The fractionation of oxygen isotopes between carbonate and water, $\alpha_{c\text{-}w}$, is calculated for the experimental temperature of 175°C. We use separate temperature-$\alpha_{c\text{-}w}$ relationships for aragonite (Kim et al., 2007) and calcite (Kim & O'Neil, 1997). Equation 5 is also built upon an assumption that internal water is a homogeneous, equally reactive mass.

For a given pair of heated and unheated samples, the CEF value can be calculated independently of $\delta^{18}O$ using clumped isotopes. This is done by normalizing the change in Δ_{47} value after heating, compared to the expected value at thermal equilibrium with the experimental temperature.

$$\text{CEF}[\Delta_{47}, T] = \frac{\Delta^{\text{heated}}_{47} - \Delta^{\text{initial}}_{47}}{\Delta^{\text{equilibrium}}_{47}(\text{T}) - \Delta^{\text{initial}}_{47}} \tag{6}$$

The Δ_{47} and Δ_{48} values for the CEF are assumed to be at equilibrium (following Equations 2 and 3 respectively), an assumption which will be tested experimentally in Section 4.2. Mixtures of CEF and unaltered material are

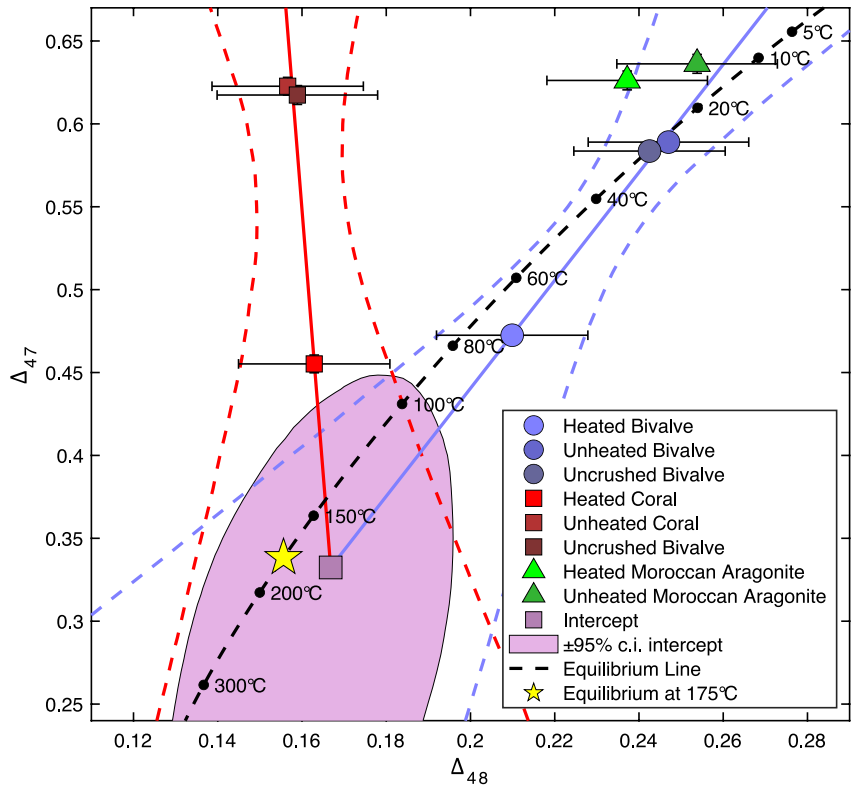

Figure 3. Dual clumped isotope data for unheated, heated and uncrushed samples from the 175°C heating experiments. Linear regression through bivalve and coral data is extrapolated to estimate heated endmember Δ_{47} and Δ_{48} values. Dashed lines represent the 95% confidence interval for linear regression. Extrapolated intercept of coral and bivalve lines shown within shaded region representing the region of 95% confidence, calculated using a Monte-Carlo approach based on re-sampling measured data. Error bars on samples represent the fully propagated 95% confidence interval as given in Table 1.

computed using isotopologue mixing which accounts for non-linear mixing effects in Δ_{47} and Δ_{48} (Defliese & Lohmann, 2015), considering that water-carbonate interaction only affects $\delta^{18}O$, but not $\delta^{13}C$.

3. Results

All isotopic results are presented in Table 1.

3.1. 175°C Aragonite Heating Experiments

Each sample's carbonate clumped isotope composition was typically measured with 8–9 replicates, yielding fully error propagated 2SE uncertainties of 0.005–0.010‰ for Δ_{47} and 0.017–0.032‰ for Δ_{48} (Table 1, Figure 3). Fluid inclusion δ^2H values published by Nooitgedach, van der Lubbe, Ziegler, and Staudigel (2021) are shown in Table 1, these show no significant change during heating for Moroccan aragonite and the bivalve, and a positive change for the belemnite and coral samples. Results for fluid/carbonate $\delta^{18}O$ measurements and corresponding paleotemperatures are also presented in Table 1. The results for $T\alpha_{c\text{-}w}$ and dual-clumped isotopes are presented alongside CEF model results in Figure 2. The CEF model shows decoupled change in $T\alpha_{c\text{-}w}$ and $T\Delta_{47}$ values during early recrystallization with low water/rock ratios, and coupled change in these parameters in more open-system models.

3.2. Belemnite Heating Experiments

Due to the lower availability of sample material, not all heated Jurassic belemnites were analyzed to the same degree of precision as the other measurements presented here. The change in the corresponding Δ_{48} values

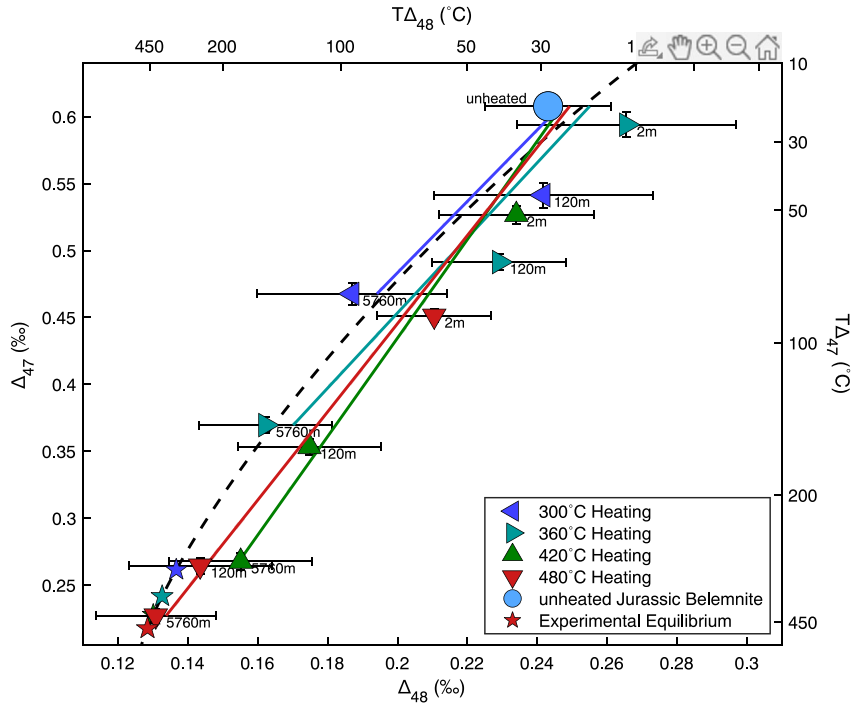

Figure 4. Heated Jurassic belemnite results. Δ_{47} (*y*-axis) and Δ_{48} (*x*-axis) values for Jurassic Wiltshire belemnites, results for each heating experiment (300°C–480°C) are shown with separate colors and symbols, the equilibrium Δ_{47}/Δ_{48} value for each experimental temperature is shown as a star of the appropriate color on the dashed "equilibrium line" (Fiebig et al., 2021). Error bars represent the fully propagated 95% confidence intervals from Table 1. Lines show the linear regression for each temperature experiment, weighted by the number of replicates for each point.

covaried significantly with Δ_{47} values in a linear fashion, and remained very close to the Fiebig et al. (2021) equilibrium relationship (Figure 4).

Cretaceous belemnites from Norfolk were heated to 360°C for 2 hr and show an indistinguishable change in Δ_{47} and Δ_{48} to that reported for the Jurassic sample (Table 1), the $T\alpha_{c\text{-}w}$ for these samples is within confidence the same as $T\Delta_{47}$ and $T\Delta_{48}$ for the unheated material (Figure 5a), and the heated belemnites' fluid inclusions $\delta^{18}O$ values were offset by ~20‰ from unheated values (Table 1). Hydrogen isotopes in the heated sample were more positive by approximately 30‰ compared to the unheated belemnites (Table 1).

3.3. Belemnite Drilling Experiments

Four Cretaceous belemnite specimens were analyzed for dual-clumped isotopes that were made into a powder using a hand-drill or a mortar and pestle. Δ_{47} values ranged between 0.600 and 0.609‰ for belemnites sampled using a mortar and pestle, drilled values ranged between 0.575 and 0.593‰ (Figure 6a). Δ_{48} values ranged between 0.246 and 0.269‰ for belemnites sampled using a mortar and pestle, drilled values ranged between 0.245 and 0.259‰ (Figure 6b).

4. Discussion

4.1. $T\alpha_{c\text{-}w}$, Δ_{47}, Δ_{48}, and δ^2H Values of Unheated Samples

The *Hippopus* bivalve Δ_{47} and Δ_{48} values plot on the equilibrium Δ_{47}/Δ_{48} line, and yield a $T\Delta_{47}$ of 28 ± 2°C (Figure 3). Belemnites also exhibit Δ_{47}–Δ_{48} values indistinguishable from equilibrium, yielding temperatures which are in agreement with the measured fluid inclusion temperatures (Table 1, Figure 5). *Montastraea* coral plots significantly above the equilibrium line (Figure 3), an observation made by previous workers for other warm-water coral species attributed to kinetics associated with the absorption of metabolic CO_2 into the calcifying fluid (Bajnai et al., 2020; Davies et al., 2022). Estimated paleotemperatures from $\alpha_{c\text{-}w}$ and Δ_{47}/Δ_{48} are compared with one another in Figure 5 in a $\alpha_{c\text{-}w}\Delta_{47}\Delta_{48}$ (ADD) diagram, this is accomplished by subtracting the

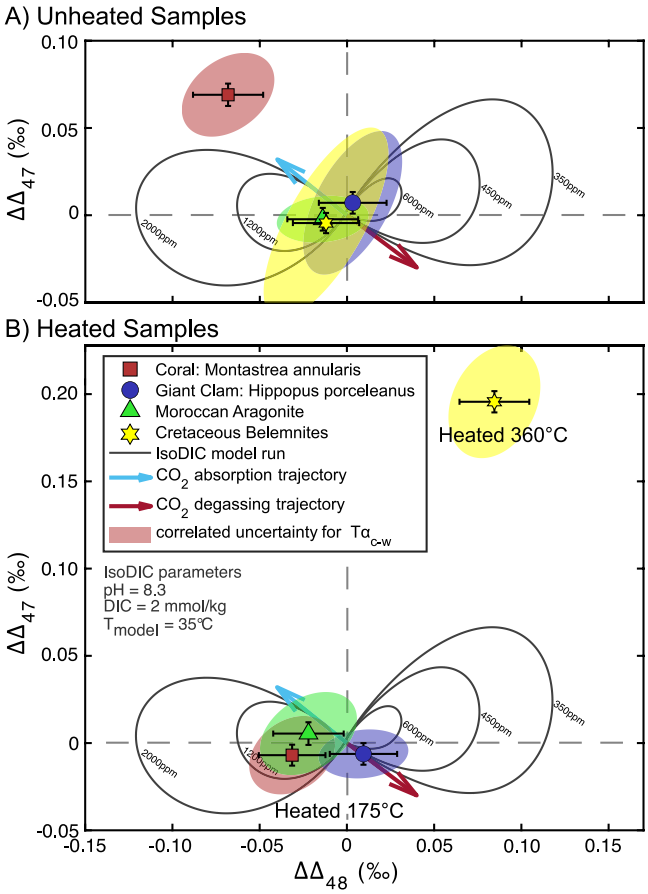

Figure 5. $\alpha_{c\text{-}w}\Delta_{47}\Delta_{48}$ (ADD) diagram showing the Δ_{47} and Δ_{48} values, normalized to apparent equilibrium temperature calculated using internal fluids and carbonate $\delta^{18}O$ values ($T\alpha_{c\text{-}w}$). Model results for CO_2 degassing and absorption (IsoDIC: Guo, 2020) are shown as black lines behind data. Mean values are shown as filled symbols, with error bars for Δ_{47} and Δ_{48} values representing 95% confidence intervals, correlated uncertainty from $T\alpha_{c\text{-}w}$ is shown as a colored region behind points, defined as an ellipse containing to solutions to 95% of Monte Carlo simulations centered around the mean value. (a) Results from unheated bivalve, coral, belemnite and Moroccan aragonite. (b) Results from heated bivalve, coral, belemnite and Moroccan aragonite.

equilibrium Δ_{47} and Δ_{48} values for $T\alpha_{c\text{-}w}$ from measured Δ_{47} and Δ_{48} values and plotting the residuals as $\Delta\Delta_{47}$ and $\Delta\Delta_{48}$ values. This way it is possible to visualize the direction and magnitude by which measured values differ from concordant equilibrium between all three (paleo)thermometers. Accounting for the fluid inclusion's analytical uncertainty will only ever increase the absolute uncertainty of paleotemperature estimates. Propagating the uncertainty of $T\alpha_{c\text{-}w}$ values into the ADD diagram results in a correlated uncertainty in the $\Delta\Delta_{47}$ and $\Delta\Delta_{48}$ values, this error propagation is calculated using a Monte-Carlo approach ($N = 1{,}000$ permutations).

Samples in this ADD diagram whose $\Delta\Delta_{47}$ and $\Delta\Delta_{48}$ values plot near the origin are at equilibrium with respect to all three paleothermometers. The correlated uncertainty of $\Delta\Delta_{47}$ and $\Delta\Delta_{48}$ from $T\alpha_{c\text{-}w}$ is shown as a colored ellipse behind the sample marker, the ellipses contain 95% of Monte-Carlo iterations. By comparing measured $\Delta\Delta_{47}$ and $\Delta\Delta_{48}$ values with IsoDIC models for CO_2 absorption and degassing (Guo, 2020), the processes governing disequilibrium compositions can be constrained. The result of this analysis shows within uncertainty the same deviation of $\Delta\Delta_{47}$ and $\Delta\Delta_{48}$ values for corals observed by Davies et al. (2022) and (Bajnai et al., 2020), thus indicating that the absorption of metabolic CO_2 into the calcification space plays an important role in governing coral skeleton composition, which has also been shown to significantly affect $\delta^{13}C$ and $\delta^{18}O$ (Chen et al., 2018). Importantly, this observation could be made without a priori knowledge of crystallization temperature. The ADD diagram shows no measurable disequilibrium behavior for bivalves, Moroccan aragonite and belemnites.

Unheated Moroccan aragonite is slightly above the equilibrium line (Figure 3), but within uncertainty indistinguishable from equilibrium. Its Δ_{47} value reflects a formation temperature of 11°C ± 2°C. Nooitgedach, van der Lubbe, Ziegler, and Staudigel (2021) and Chen et al. (2019) both reported $T(\Delta_{47})$ of 22.3°C ± 15.5°C and 16°C ± 5°C for samples of Moroccan/Tazouta aragonite. Our $T(\Delta_{47})$ is within their uncertainties, although generally cooler and with a greater precision such that the previously measured temperatures are outside our 95% confidence intervals. Our measurements also agree with the $T\alpha_{c\text{-}w}$ of 10.6°C ± 1.9°C calculated with fluid and carbonate $\delta^{18}O$ values (Figure 5a). These temperatures, coupled with the low $\delta^{18}O_{fluid}$ values on the global meteoric water line, indicate a near-surface, possibly meteoric, origin for Tazouta aragonite. Unheated belemnites are indistinguishable from Δ_{47}/Δ_{48} equilibrium, an observation supported by previous measurement of a belemnite rostrum by Bajnai et al. (2020).

The δ^2H values of bivalve, coral and abiogenic aragonite samples were first presented by Nooitgedach, van der Lubbe, Ziegler, and Staudigel (2021), and the belemnite compositions are presented here for the first time. As stated by Nooitgedach, van der Lubbe, Ziegler, and Staudigel (2021), it is unclear what the geochemical significance of hydrogen isotope ratios in internal water of biogenic materials is. While the Moroccan aragonite is clearly near the global meteoric water line, the biogenic materials fall well below this line even though the $\delta^{18}O$ values are consistent with modern seawater (see Figure 2 of Nooitgedach, van der Lubbe, Ziegler, & Staudigel, 2021). This indicates that the internal water released in the crusher apparatus may not simply be trapped seawater, but may have undergone some exchange with hydrogen-rich organic molecules (Figure 1c) either during biomineralization or analysis.

4.2. Direct Heating Experiments

The alteration of Δ_{47} and Δ_{48} values of belemnites and bivalves follows the equilibrium line during the heating experiments (Figure 4), suggesting that in a closed system, it is difficult to unambiguously identify the effects of heating, especially for samples whose initial compositions are indistinguishable from the equilibrium line. The

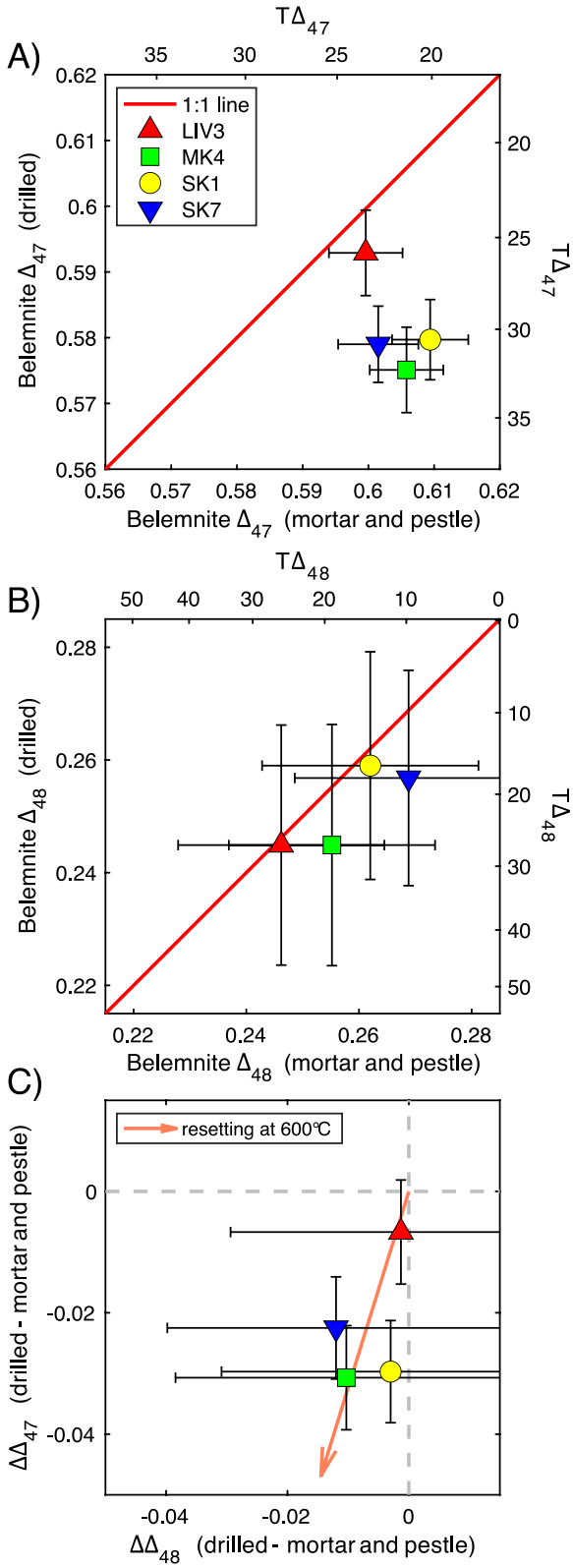

Figure 6. Comparison of Δ_{47} and Δ_{48} values in belemnites sampled using a drill and a mortar and pestle. (a) Comparison of Δ_{47} values. (b) Comparison of Δ_{48} values. (c) Comparison of change in Δ_{47} and Δ_{48} values with vector showing expected change due to heating at 600°C.

modified mass-balance CEF model yields specific predictions for the behavior of Δ_{47} and Δ_{48} in systems with differing water/carbonate ratios, with low ratios yielding nearly linear trajectories in Δ_{47}/Δ_{48} space, and higher water/carbonate ratios departing from this line due to non-linear mixing effects (Figure 2b). This is possible because non-linear mixing effects in Δ_{47} require a difference in both $\delta^{13}C$ and $\delta^{18}O$ (Defliese & Lohmann, 2015) whereas Δ_{48} displays non-linear mixing even if there is only a difference in $\delta^{18}O$. The non-linear mixing trajectories for clumped isotopes exist due to the way in which Δ_{47} and Δ_{48} are defined (Equation 1), wherein the stochastic denominator term is calculated as the product of multiple singly-substituted isotopologues, whereas the numerator considers predominantly the abundance of a single multiply-substituted isotopologue, a more complete description of this behavior is available in Supporting Information S1. Because the CEF model assumes no fractionation of carbon isotopes, only Δ_{48} is expected to show non-linear mixing. This assumption could only be violated if an additional source of carbon were available or if CO_2 were expelled during heating, thus violating the closed-system assumption of this model. This suggests that Δ_{48} would be a useful tool for calculating the extent of hydrothermal alteration in systems with a larger water/carbonate ratio.

The CEF evolution models for low water/rock ratio effectively describe the Δ_{47} and Δ_{48} values of the heated samples, and using the equilibrium value for the 175°C heating experiment appears to be reasonable. Because the unheated coral specimen possessed disequilibrium Δ_{47} and Δ_{48} values, and the bivalve's were indistinguishable from equilibrium, it is also possible to extrapolate through their heated and unheated values and calculate the Δ_{47} and Δ_{48} value of the thermally altered carbonate end-member. Extrapolating through the heated and unheated samples for both specimens yield an intercept that is statistically indistinguishable from equilibrium at the experimental temperature of 175°C (Figure 3), thus supporting the assumption that the CEF endmember can be considered to be at thermodynamic equilibrium. This extrapolation exercise demonstrates that even if the heating temperature were unknown, it would be mathematically possible to utilize dual-clumped isotope analyses to reconstruct peak heating temperatures if multiple carbonate allochems with initially disequilibrated states are sampled in a given stratum, although the uncertainty inherent in such estimations would be undoubtedly high with the currently available resolution of Δ_{48} measurement. The belemnite data also appear to follow this trend (Figure 4), although the differences in peak heating temperature cannot be as easily determined in the same way because the unheated belemnite was initially close to the equilibrium line, and the heated equilibrium values are too similar to one another in Δ_{47}/Δ_{48} space. Our analyses of Cretaceous belemnites confirm the interpretations of Looser et al. (2023), highlighting that internal fluids play an important role in resetting belemnite Δ_{47} values, as fluid and carbonate $\delta^{18}O$ values have notably changed during heating.

The CEF model does purely describe oxygen isotope exchange between carbonate and water, and thus not predict any change in $\delta^{2}H$. However, some samples do show a shift toward more positive $\delta^{2}H$ values during heating (Table 1), thus some other process must be at play in addition to the exchange between carbonate and internal water during heating. The coral and belemnite samples show a significant ($p < 0.05$) change in $\delta^{2}H$ during heating, and the bivalve and Tazouta aragonite do not (See figure two from Nooitgedach, van der Lubbe, Ziegler, & Staudigel, 2021). Fractional evaporation of water during heating is a plausible candidate for correlated positive change in $\delta^{18}O$

and δ^2H values, as was observed in coral and belemnite samples. This correlation is understandable if the lighter isotopes of hydrogen and oxygen escape as samples are heated. This behavior in more permeable biogenic materials is unsurprising, and has been discussed previously by de Graaf et al. (2022).

4.3. Fingerprinting Alteration in an ADD Diagram

The observation that thermal alteration at lowermost water/carbonate ratios falls on a near-linear mixing line alongside correlated changes in $\delta^{18}O$ of fluids and carbonates, largely supports the predictions of the CEF model. This does, however, mean that altered samples' Δ_{47} and Δ_{48} values may still yield values concordant with the equilibrium relationship between these proxies despite the alteration, especially if the primary material was near equilibrium (e.g., belemnites shown in Figure 4 and bivalve samples shown in Figure 3). Thus, identifying this closed-system resetting would require an additional metric that has a different sensitivity to thermal resetting. Fluid inclusions present a tempting solution to this problem, as the CEF model predicts that they should be far more sensitive to heating than clumped isotopes (Nooitgedacht, van der, Lubbe, de, et al., 2021), this illustrated in Figure 2 by the rapid change in $\alpha_{c\text{-}w}$ with minimal change in Δ_{47} in models with high carbonate fractions (F_c). Analysis of fluid inclusions and dual-clumped isotopes yields three independent estimates of apparent crystallization temperature, making it a unique tool for quantifying disequilibrium or kinetic effects during mineralization, even when the "true" crystallization temperature is unknown.

Figure 5b shows an ADD diagram for the heated bivalve, coral, Tazouta aragonite, and belemnite analyses. The heated belemnite shows a clear departure from the origin, which gives hope that this method may be applicable to fossil samples. It does not, however, show any disequilibrium effect for the bivalve, and shows only a small deviation for coral D48-values consistent with the inherited disequilibrium from the unheated corals. The concordant $T\alpha_{c\text{-}w}$ and $T\Delta_{47}$ values for these samples are shown in Figure 5b. As a consequence of this agreement between paleothermometers, it would be impossible to identify the 50°C difference in $T\Delta_{47}$ and $T\alpha_{c\text{-}w}$ between heated and unheated samples (Table 1) using this criterion. This discrepancy is possibly due to the presence of multiple internal water populations in modern corals and bivalves. On the contrary, due to oxidation of organic matter during deposition and burial, organic-associated water might be less abundant in the belemnites.

4.4. Multiple Internal Water Populations

The CEF model as originally presented by Nooitgedacht, van der, Lubbe, de, et al. (2021) and Nooitgedach, van der Lubbe, Ziegler, and Staudigel (2021) does not reasonably describe the fluid inclusion data for the heated biogenic aragonite, their Δ_{47} and $\alpha_{c\text{-}w}$ values require water fractions greater than 1, which is mathematically permitted, but physically impossible in a closed system (Figure 2a). The "impossible" values for Δ_{47} and $\alpha_{c\text{-}w}$ would be permitted in an open system, where external water is supplied, but this is impossible in a dry-heating scenario. This behavior would be expected, however, if different populations of water within the sample have different reactivities, possibly organic-associated and "classic" fluid inclusions as shown in Figure 1d. If organic-associated water is likely to exchange, and classic fluid inclusions are otherwise unreactive (as the unchanged heated Moroccan aragonite data suggests), then the departure from the standard CEF model would be understandable. If water is comprised of a reactive and non-reactive water phase (perhaps resembling the organic and native water shown in Figure 1d), then Equation 5 can be modified to account for this exchangeable water fraction (WEF).

$$ {}^{18}R^{\text{heated}}_{\text{WEF}} = \frac{{}^{18}R^{\text{initial}}_{\text{carbonate}} * F_c * \text{CEF} + {}^{18}R^{\text{initial}}_{\text{fluid}} * (1 - F_c) * \text{WEF}}{F_c * \text{CEF} + (1 - F_c) * \alpha_{c-w}(T) * \text{WEF}} \quad (7) $$

Note that when WEF = 1, Equation 7 is identical to Equation 5.

By adjusting the mass-balance model in Equation 5 to allow for variability in the quantity of exchangeable water, as shown in Equation 7, such that a fraction of water does not exchange, then variability in this "Water Exchange Fraction" (WEF) can fully explain the observed alpha values (Figure 2a), while still allowing for the F_c values suggested by the Δ_{47}/Δ_{48} model (Figure 2b). The variable WEF models are nearly indistinguishable from the $F_c = 0.98$ model in Δ_{47}/Δ_{48} space, although they are distinct (as shown in the inset of Figure 2b), due to the small differences in the $\delta^{18}O$ value of the heated carbonate fraction resulting from less water being available for exchange. The presence of multiple, distinct, water masses in biogenic carbonates is unsurprising, as water can be associated with organic components, integral to crystal structures or present as "true" fluid inclusions (Gaffey, 1988).

4.5. Does the Heat of the Crusher Apparatus Facilitate Internal Fluid-Carbonate Exchange?

Published methods for fluid inclusion analysis requires heating samples to temperatures over 100°C. Experiments at higher temperatures have observed fluid-carbonate exchange in speleothems and biogenic samples (Nooitgedach, van der Lubbe, Ziegler, & Staudigel, 2021; Ritter et al., 2017; Uemura et al., 2019), but no firm lower limit exists on when this fluid-carbonate exchange ceases to occur. Geochemical analysis of exhumed carbonate veins indicated that this process can occur, likely at a slow rate, at temperatures well below the boiling point of water (Nooitgedacht, van der, Lubbe, de, et al., 2021). Early work on speleothems recommended heating up to 150°C (Dennis et al., 2001), although more recent publications revised this to 110°C, just above boiling point at atmospheric pressure (Arienzo et al., 2013; Nooitgedach, van der Lubbe, Ziegler, & Staudigel, 2021; Vonhof et al., 2006). Given the demonstrated susceptibility of biogenic materials to heating-induced fluid-carbonate exchange, it is reasonable to suspect that this process could affect the fluid inclusion and to a lesser extent the carbonate $\delta^{18}O$ values. If found to be true, this accusation would invalidate any attempted measurement of $\delta^{18}O$ of biogenic carbonate-associated fluid inclusions using this method, and thus it is critical that we evaluate it.

Results from our high precision clumped isotope analyses indicate no evidence for carbonate-fluid exchange at 110°C during the 1–2 hr samples spent in the crusher apparatus. There is no significant difference in Δ_{47} or Δ_{48} values between samples which were analyzed for fluid inclusions ("unheated") and those that were simply crushed manually ("uncrushed") (Table 1; Figure 3). Similarly, the Moroccan aragonite shows minimal change at 175°C (Figure 3). The CEF value, as estimated using Δ_{47}, makes a useful metric for the extent of this internal exchange. When calculated for the "crushed" versus "uncrushed" bivalve and coral specimens, CEF values of 0.019 ± 0.059 and 0.022 ± 0.076 (95% confidence, propagated from uncertainty in Δ_{47} measurements) are obtained, making them indistinguishable from zero. The heated Moroccan aragonite (heated to 175°C) also had a near-zero CEF value (0.034 ± 0.056), a good indication that the heat of the crusher apparatus would not facilitate exchange with the fluid inclusions at 110°C.

These results should give confidence to workers using this method, but the possibility for fluid-carbonate exchange cannot be definitively ruled out in all future contexts, in particular for biogenic carbonates. Future workers are still advised to minimize the time samples are stored at high temperatures prior to analysis.

4.6. Does Drilling Samples Affect Clumped Isotope Paleotemperatures?

The heat associated with micro-drilling is known to affect the $\delta^{18}O$ and Δ_{47} values of archives (Foster et al., 2008; Moon et al., 2021; Staudigel & Swart, 2016; Waite & Swart, 2015). These previous works have focused on aragonitic archives, which have the useful property that the heat of the drill would also convert aragonite to calcite, and thus correlation between the loss of aragonite and a change in isotopic composition provide additional support for the hypothesis. This does not, however, mean that calcite specimens are exempt from this effect, just that it cannot be as easily quantified. Our belemnite results demonstrate this; sub-samples of belemnite calcite taken with a hand drill (PROXXON D-54343), on the lowest speed setting, yield significantly higher Δ_{47} values (y-axis on Figure 6a) which translate to warmer temperatures than samples from the same specimen ground in a mortar and pestle (x-axis on Figure 6a). There is no significant change in Δ_{48} values (Figure 6b), however this is to be expected as the temperature sensitivity of Δ_{48} is less than that of Δ_{47} (Figure 6c), and thus changes in Δ_{48} would require significantly greater degrees of alteration to become apparent.

Experiments with drilling have shown minimal effect of drills on the isotopic compositions of abiogenic carbonate archives such as aragonitic speleothems (Staudigel & Swart, 2016), or calcite speleothems (Spötl and Mattey, 2006). Experiments conducted by Nooitgedach, van der Lubbe, Ziegler, and Staudigel (2021) show that abiogenic carbonates are less prone to re-equilibration with internal fluids at elevated temperatures (corresponding to low CEF values in Equations 5 and 7). Although exchange of carbon and oxygen between carbonate and atmospheric CO_2 occurs at elevated temperatures (Staudigel & Swart, 2016) and thus may also occur during drilling, experiments where archives were drilled in argon atmospheres have shown indistinguishable changes in $\delta^{18}O$ (Gill et al., 1995). From this, we can argue that the resetting of clumped isotopes and $\delta^{18}O$ values during drilling is the same process observed during our direct heating experiments, where the heat of a drill bit facilitates these exchange reactions. Although direct measurements of drill bit temperatures are rare, some experimental work has been conducted in the manufacturing industry and temperatures of ~600°C are not unreasonable (Beno & Hulling, 2012). The expected slope for Δ_{47} and Δ_{48} resetting at 600°C is shown in Figure 6c, however it would

be difficult to distinguish resetting at lower temperatures by slope alone using this method due to the relatively small differences in equilibrium value at these temperatures and the larger uncertainties in Δ_{48} measurements. Experiments conducted by Staudigel & Swart, (2016) thermally converted aragonite to calcite at temperatures of 300°C–425°C; extrapolating these results with an Arrhenius relationship indicates that the conversion should occur in less than 1 s at 600°C.

It is known that drill heating, and thus alteration, can be minimized by using slower drill RPM (Baci & Ozcelik, 2007; Moon et al., 2021), however we urge researchers whose goal is to conduct accurate isotopic measurement to avoid drilling biogenic samples wherever possible, regardless of mineralogy. If drilling cannot be avoided, for instance in cases where high temporal precision is necessary from an archive being sampled with a micro-drill, an experiment like the one presented in Figure 6 should be conducted to test the suitability of a given approach. If drilling can be proven to be indistinguishable from mortar and pestle in a given case, then sclerochronological data from the same specimen could be considered unaffected by thermal resetting.

5. Conclusions

Exchange between carbonate and internal fluids appears to be an equilibrium-driven process at elevated temperatures, this exchange is limited by the fractions of carbonate and water available for reaction. Closed-system exchange results in near-linear correlation of Δ_{47} and Δ_{48} values which behave as a simple mixing model between primary values and the predicted values for clumped isotope equilibrium. This co-linearity is not expected in systems where larger quantities of water are available, due to non-linear mixing effects on Δ_{48}. We demonstrate that analysis of fluid inclusions and dual-clumped isotopes provide a useful tool for exploring both nature of initial equilibrium/disequilibrium behavior during initial mineral formation, as well as identifying the effects of thermal alteration. Lastly, we implemented high-precision dual-clumped isotope measurements on samples treated using different common laboratory techniques to evaluate if they facilitate exchange between carbonate and internal fluids; we find that the ∼110°C heat of a crusher apparatus used for fluid inclusion analysis does not facilitate exchange over the duration of typical fluid inclusion analysis, demonstrating its suitability for analyzing the internal fluids in biogenic carbonates. Conversely, we demonstrate that belemnites' clumped isotope compositions are significantly affected by sampling with a hand-drill, and we propose a simple test wherein drilled samples are compared to samples ground with mortar and pestle. Because sub-sampling archives with a drill is an indisputably useful technique for reconstructing climate variability, we present this test as a simple means of validating the suitability of any sampling technique.

Conflict of Interest

The authors declare no conflicts of interest relevant to this study.

Data Availability Statement

Supplementary files including averaged and individual clumped isotope analyses are available as a Supporting Information S1 to this text. Additional discussion on isotopologue mixing and error propagation is available as a Supporting Information S2 document. The supplementary datasets and code are permanently archived via Zenodo accessible via the DOI https://doi.org/10.5281/zenodo.7565557.

Acknowledgments
Weifu Guo is thanked for the use of his IsoDIC model. Sven Hofmann and Suzan Verdegaal are graciously thanked for technical support. The research was funded through DFG grant FI-948/13-1. Two anonymous reviewers are thanked for their helpful contributions to this manuscript. Open Access funding enabled and organized by Projekt DEAL.

References

Arienzo, M. M., Swart, P. K., & Vonhof, H. B. (2013). Measurement of $\delta^{18}O$ and $\delta^{2}H$ values of fluid inclusion water in speleothems using cavity ring-down spectroscopy compared with isotope ratio mass spectrometry. *Rapid Communications in Mass Spectrometry*, *27*(23), 2616–2624. https://doi.org/10.1002/rcm.6723

Baci, E., & Ozcelik, B. (2007). Influence of cutting parameters on drill bit temperature in dry drilling of AISI 1040 steel material using statistical analysis. *Industrial Lubrication & Tribology*, *59*(4), 186–193. https://doi.org/10.1108/00368790710753581

Bajnai, D., Guo, W., Spotl, C., Coplen, T. B., Methner, K., Loffler, N., et al. (2020). Dual clumped isotope thermometry resolves kinetic biases in carbonate formation temperatures. *Nature Communications*, *11*, 1–9. https://doi.org/10.1038/s41467-020-17501-0

Banner, J. L., & Hanson, G. N. (1990). Calculation of simultaneous isotopic and trace element variations during water-rock interaction with applications to carbonate diagenesis. *Geochimica et Cosmochimica Acta*, *54*(11), 3123–3137. https://doi.org/10.1016/0016-7037(90)90128-8

Beno, T., & Hulling, U. (2012). Measurement of cutting edge temperature in drilling. *Procedia CIRP*, *3*, 531–536. https://doi.org/10.1016/j.procir.2012.07.091

Bernasconi, S. M., Daëron, M., Bergmann, K. D., Bonifacie, M., Meckler, A. N., Affek, H. P., et al. (2021). *InterCarb: A community effort to improve interlaboratory standardization of the carbonate clumped isotope thermometer using carbonate standards* (Vol. 22, pp. 1–25). Geochemistry, Geophysics, Geosystems. 10.1029/2020GC009588

Brenner, D. C., Passey, B. H., & Stolper, D. A. (2018). Influence of water on clumped-isotope bond reordering kinetics in calcite. *Geochimica et Cosmochimica Acta*, *224*, 42–63. https://doi.org/10.1016/j.gca.2017.12.026

Chen, S., Gagnon, A. C., & Adkins, J. F. (2018). Carbonic anhydrase, coral calcification and a new model of stable isotope vital effects. *Geochimica et Cosmochimica Acta*, *236*, 179–197. https://doi.org/10.1016/j.gca.2018.02.032

Chen, S., Ryb, U., Piasecki, A. M., Lloyd, M. K., Baker, M. B., & Eiler, J. M. (2019). Mechanism of solid-state clumped isotope reordering in carbonate minerals from aragonite heating experiments. *Geochimica et Cosmochimica Acta*, *258*, 156–173. https://doi.org/10.1016/j.gca.2019.05.018

Daëron, M. (2021). Full propagation of analytical uncertainties in Δ_{47} measurements. *Geochemistry, Geophysics, Geosystems*, *22*(5), e2020GC009592. https://doi.org/10.1029/2020gc009592

Davies, A. J., Guo, W., Bernecker, M., Tagliavento, M., Raddatz, J., Gischler, E., et al. (2022). Dual clumped isotope thermometry of coral carbonate. *Geochimica et Cosmochimica Acta*, *338*, 66–78. https://doi.org/10.1016/j.gca.2022.10.015

Defliese, W. F., & Lohmann, K. C. (2015). Non-linear mixing effects on mass-47 CO_2 clumped isotope thermometry: Patterns and implications. *Rapid Communications in Mass Spectrometry*, *29*(9), 901–909. https://doi.org/10.1002/rcm.7175

de Graaf, S., Vonhof, H. B., Reijmer, J. J., Feenstra, E., Mienis, F., Prud'Homme, C., et al. (2022). Analytical artefacts preclude reliable isotope ratio measurement of internal water in coral skeletons. *Geostandards and Geoanalytical Research*, *46*(3), 563–577. 10.1111/ggr.12445

de Graaf, S., Vonhof, H. B., Weissbach, T., Wassenburg, J. A., Levy, E. J., Kluge, T., & Haug, G. H. (2020). A comparison of IRMS and CRDS techniques for isotope analysis of fluid inclusion water. *Rapid Communications in Mass Spectrometry*, *34*(16), e8837. https://doi.org/10.1002/rcm.8837

Dennis, P. F., Rowe, P. J., & Atkinson, T. C. (2001). The recovery and isotopic measurement of water from fluid inclusions in speleothems. *Geochimica et Cosmochimica Acta*, *65*(6), 871–884. https://doi.org/10.1016/s0016-7037(00)00576-7

Fiebig, J., Bajnai, D., Löffler, N., Methner, K., Krsnik, E., Mulch, A., & Hofmann, S. (2019). Combined high-precision Δ_{48} and Δ_{47} analysis of carbonates. *Chemical Geology*, *522*, 186–191. https://doi.org/10.1016/j.chemgeo.2019.05.019

Fiebig, J., Daëron, M., Bernecker, M., Guo, W., Schneider, G., Boch, R., et al. (2021). Calibration of the dual clumped isotope thermometer for carbonates. *Geochimica et Cosmochimica Acta*, *312*, 235–256. https://doi.org/10.1016/j.gca.2021.07.012

Foster, L. C., Andersson, C., Høie, H., Allison, N., Finch, A. A., & Johansen, T. (2008). Effects of micromilling on $\delta^{18}O$ in biogenic aragonite. *Geochemistry, Geophysics, Geosystems*, *9*(4), 1–6. https://doi.org/10.1029/2007gc001911

Gaffey, S. J. (1988). Water in skeletal carbonates. *Journal of Sedimentary Petrology*, *58*, 397–414.

Gaffey, S. J., Kolak, J. J., & Bronnimann, E. C. (1991). Effects of drying, heating, annealing, and roasting on carbonate skeletal material, with geochemical and diagenetic implications. *Geochimica et Cosmochimica Acta*, *55*(6), 1627–1640. https://doi.org/10.1016/0016-7037(91)90134-q

Ghosh, P., Adkins, J., Affek, H., Balta, B., Guo, W., Schauble, E. A., et al. (2006). ^{13}C–^{18}O bonds in carbonate minerals: A new kind of paleothermometer. *Geochimica et Cosmochimica Acta*, *70*(6), 1439–1456. https://doi.org/10.1016/j.gca.2005.11.014

Gill, I., Olson, J. J., & Hubbard, D. K. (1995). Corals, paleotemperature records, and the aragonite-calcite transformation. *Geology*, *23*(4), 333–336. https://doi.org/10.1130/0091-7613(1995)023<0333:cprata>2.3.co;2

Guo, W. (2020). Kinetic clumped isotope fractionation in the DIC-H_2O-CO_2 system: Patterns, controls, and implications. *Geochimica et Cosmochimica Acta*, *268*, 230–257. https://doi.org/10.1016/j.gca.2019.07.055

Hemingway, J. D., & Henkes, G. A. (2021). A disordered kinetic model for clumped isotope bond reordering in carbonates. *Earth and Planetary Science Letters*, *566*, 116962. https://doi.org/10.1016/j.epsl.2021.116962

Henkes, G. A., Passey, B. H., Grossman, E. L., Shenton, B. J., Pérez-Huerta, A., & Yancey, T. E. (2014). Temperature limits for preservation of primary calcite clumped isotope paleotemperatures. *Geochimica et Cosmochimica Acta*, *139*, 362–382. https://doi.org/10.1016/j.gca.2014.04.040

Hill, P. S., Tripati, A. K., & Schauble, E. A. (2014). Theoretical constraints on the effects of pH, salinity, and temperature on clumped isotope signatures of dissolved inorganic carbon species and precipitating carbonate minerals. *Geochimica et Cosmochimica Acta*, *125*, 610–652. https://doi.org/10.1016/j.gca.2013.06.018

Kim, S. T., & O'Neil, J. R. (1997). Equilibrium and nonequilibrium oxygen isotope effects in synthetic carbonates. *Geochimica et Cosmochimica Acta*, *61*(16), 3461–3475. https://doi.org/10.1016/s0016-7037(97)00169-5

Kim, S. T., O'Neil, J. R., Hillaire-Marcel, C., & Mucci, A. (2007). Oxygen isotope fractionation between synthetic aragonite and water: Influence of temperature and Mg^{2+} concentration. *Geochimica et Cosmochimica Acta*, *71*(19), 4704–4715. https://doi.org/10.1016/j.gca.2007.04.019

Looser, N., Petschnig, P., Hemmingway, J., Fernandez, A., Grafulha-Morales, L., Perez-Huerta, A., et al. (2023). Thermally-induced clumped isotope resetting in belemnite and optical calcites: Towards material-specific kinetics. *Geochimica et Cosmochimica Acta*. https://www.sciencedirect.com/science/article/pii/S001670372300145X?via%3Dihub

Moon, L. R., Judd, E. J., Thomas, J., & Ivany, L. C. (2021). Out of the oven and into the fire: Unexpected preservation of the seasonal $\delta^{18}O$ cycle following heating experiments on shell carbonate. *Palaeogeography, Palaeoclimatology, Palaeoecology*, *562*, 110115. https://doi.org/10.1016/j.palaeo.2020.110115

Nooitgedacht, C. W., van der Lubbe, H. J. L., de Graaf, S., Ziegler, M., Staudigel, P. T., & Reijmer, J. J. G. (2021). Restricted internal oxygen isotope exchange in calcite veins: Constraints from fluid inclusion and clumped isotope-derived temperatures. *Geochimica et Cosmochimica Acta*, *297*, 24–39. https://doi.org/10.1016/j.gca.2020.12.008

Nooitgedacht, C. W., van der Lubbe, H. J. L., Ziegler, M., & Staudigel, P. T. (2021). Internal water facilitates thermal resetting of clumped isotopes in biogenic aragonite. *Geochemistry, Geophysics, Geosystems*, *22*(5), 1–13. https://doi.org/10.1029/2021gc009730

Passey, B. H., & Henkes, G. A. (2012). Carbonate clumped isotope bond reordering and geospeedometry. *Earth and Planetary Science Letters*, *351–352*, 223–236. https://doi.org/10.1016/j.epsl.2012.07.021

Pederson, C., Mavromatis, V., Dietzel, M., Rollion-Bard, C., Breitenbach, S. F. M., Yu, D., et al. (2020). Variation in the diagenetic response of aragonite archives to hydrothermal alteration. *Sedimentary Geology*, *406*, 105716. https://doi.org/10.1016/j.sedgeo.2020.105716

Pedreira-Segade, U., Hao, J., Montagnac, G., Cardon, H., & Daniel, I. (2019). Spontaneous polymerization of glycine under hydrothermal conditions. *ACS Earth and Space Chemistry*, *3*(8), 1669–1677. https://doi.org/10.1021/acsearthspacechem.9b00043

Ritter, A. C., Mavromatis, V., Dietzel, M., Kwiecien, O., Wiethoff, F., Griesshaber, E., et al. (2017). Exploring the impact of diagenesis on (isotope) geochemical and microstructural alteration features in biogenic aragonite. *Sedimentology*, *64*(5), 1354–1380. https://doi.org/10.1111/sed.12356

Ryb, U., & Eiler, J. M. (2018). Oxygen isotope composition of the Phanerozoic ocean and a possible solution to the dolomite problem. *Proceedings of the National Academy of Sciences of the United States of America*, *115*(26), 6602–6607. https://doi.org/10.1073/pnas.1719681115

Spötl, C., & Mattey, D. (2006). Stable isotope microsampling of speleothems for palaeoenvironmental studies: A comparison of microdrill, micromill and laser ablation techniques. *Chemical Geology*, *235*(1–2), 48–58. https://doi.org/10.1016/j.chemgeo.2006.06.003

Staudigel, P. T., John, E. H., Buse, B., Pearson, P. N., & Lear, C. H. (2022). Apparent preservation of primary foraminiferal Mg/Ca ratios and Mg-banding in recrystallized foraminifera. *Geology*, *50*(7), 760–764. https://doi.org/10.1130/g49984.1

Staudigel, P. T., & Swart, P. K. (2016). Isotopic behavior during the aragonite-calcite transition: Implications for sample preparation and proxy interpretation. *Chemical Geology*, *442*, 130–138. https://doi.org/10.1016/j.chemgeo.2016.09.013

Staudigel, P. T., & Swart, P. K. (2019). A diagenetic origin for isotopic variability of sediments deposited on the margin of Great Bahama Bank, insights from clumped isotopes. *Geochimica et Cosmochimica Acta*, *258*, 97–119. https://doi.org/10.1016/j.gca.2019.05.002

Stolper, D. A., & Eiler, J. M. (2015). The kinetics of solid-state isotope-exchange reactions for clumped isotopes: A study of inorganic calcites and apatites from natural and experimental samples. *American Journal of Science*, *315*(5), 363–411. https://doi.org/10.2475/05.2015.01

Swart, P. K., Lu, C., Moore, E. W., Smith, M. E., Murray, S. T., & Staudigel, P. T. (2021). A calibration equation between Δ_{48} values of carbonate and temperature. *Rapid Communications in Mass Spectrometry*, *35*(17), e9147. https://doi.org/10.1002/rcm.9147

Uemura, R., Kina, Y., & Omine, K. (2019). Experimental evaluation of oxygen isotopic exchange between inclusion water and host calcite in speleothems. *Climate of the Past Discussions*, *3*, 1–18. https://doi.org/10.5194/cp-16-17-2020

Veillard, C. M. A., John, C. M., Krevor, S., & Najorka, J. (2019). Rock-buffered recrystallization of Marion Plateau dolomites at low temperature evidenced by clumped isotope thermometry and X-ray diffraction analysis. *Geochimica et Cosmochimica Acta*, *252*, 190–212. https://doi.org/10.1016/j.gca.2019.02.012

Vickers, M. L., Bernasconi, S. M., Ullmann, C. V., Lode, S., Looser, N., Morales, L. G., et al. (2021). Marine temperatures underestimated for past greenhouse climate. *Scientific Reports*, *11*(1), 19109. https://doi.org/10.1038/s41598-021-98528-1

Vonhof, H. B., Van Breukelen, M. R., Postma, O., Rowe, P. J., Atkinson, T. C., & Kroon, D. (2006). A continuous-flow crushing device for on-line δ^2H analysis of fluid inclusion water in speleothems. *Rapid Communications in Mass Spectrometry: An International Journal Devoted to the Rapid Dissemination of Up-to-the-Minute Research in Mass Spectrometry*, *20*(17), 2553–2558. https://doi.org/10.1002/rcm.2618

Waite, A. J., & Swart, P. K. (2015). The inversion of aragonite to calcite during the sampling of skeletal archives: Implications for proxy interpretation. *Rapid Communications in Mass Spectrometry*, *29*(10), 955–964. https://doi.org/10.1002/rcm.7180

Wardlaw, N., Oldershaw, A., & Stout, M. (1978). Transformation of aragonite to calcite in a marine gasteropod. *Canadian Journal of Earth Sciences*, *15*(11), 1861–1866. https://doi.org/10.1139/e78-193

Watkins, J. M., & Devriendt, L. S. (2022). A combined model for kinetic clumped isotope effects in the $CaCO_3$-DIC-H_2O system. *Geochemistry, Geophysics, Geosystems*, *23*(8), e2021GC010200. https://doi.org/10.1029/2021gc010200

Wortmann, F. J., Wortmann, G., Marsh, J., & Meinert, K. (2012). Thermal denaturation and structural changes of α-helical proteins in keratins. *Journal of Structural Biology*, *177*(2), 553–560. https://doi.org/10.1016/j.jsb.2011.09.014

Erratum

In the originally published version of this article, the Looser et al. (2022) reference was incorrect. The updated reference has now been added and this article may now be considered the authoritative version of record.